

# Noise Calculation in nano-channel diodes for Terahertz detectors application

ABDEL MAJID. MAMMERI, F.ZMAHI  
Physics of Semiconductors Laboratory  
university of Bechar  
ALGERIA  
fati\_zo\_mahi2002@yahoo.fr

L. VARANI  
Institute of electronic and systems  
University of Montpellier  
FRANCE  
fati64@live.com

**Abstract:** An analytical calculations of the intrinsic noise and Noise Equivalent Power (NEP) in the InGaAs nanochannel diode are proposed. The model based on the one dimensional Poisson equation which is derived to obtain the current-potential relation of the diode. This relation allows to calculate the admittance/impedance elements and establish the noise spectral density according to Nyquist expression. From the complex impedance of the diode, we can extract the Responsivity generated from the power signal in proportional to the power absorbed by the nanochannel diode. The analysis combine the noise spectra and the Responsivity to determine the Equivalent Noise Power (NEP) of the diode under a high frequency signal. The discussion includes the geometrical effects, the operating temperature and properties of the diode to optimize the generated power in terahertz frequency. The Responsivity and the Noise power show the appearance of resonances peaks in the terahertz domain. The analysis of the resonances improves the behavior of the nanochannel diodes for high sensitive Terahertz detectors. The analytical noise results are compared with the Mont Carlo calculations in Refs. [1], [2].

**Key-Words:** Nanochannel diodes, Terahertz (THz), resonances, Noise Equivalent Power (NEP), intrinsic noise.

## 1 Introduction

The nano-diodes have present a great potential applications in the Terahertz frequencies as detectors and emitters at room temperature [3]. In particular, the nanochannel diodes known as self-switching devices (SSDs) have shown experimentally a good Responsivity and noise properties for microwave and Terahertz detection [4], [5]. Many researchs are supported for the realization of an InGaAs nanochannel diodes in Ref. [6] then for the noise equivalent power calculation by a numerical model in Refs. [7], [4] and Mont Carlo model in Refs. [1], [2].

In this article, the noise equivalent power calculation is based on an analytical approach where the equations particularly focus thier dependance to the material parameters (relaxation rate, mobility, masse effective and permittivity), the channel geometry (length, width and carrier concentration) and the diode properties operations in applied voltage(resistance and rectifie electric current). Moreover, the analytical model can determine all the parameters related to the generated power such as the impedance  $Z(\omega)$  and therefore the resistance  $R$ , the noise spectrum ( $S_{ii}$  and  $S_{vv}$ ), the signal power in the diode  $P_{int}$  and the Responsivity  $S_{int}$ . In this case, the analytical resolution is useful to perform the high frequency generated power by discussing some param-

eters such as the impedance, the noise spectrum, the Responsivity and the noise equivalent power.

The terahertz noise spectrum (current/voltage densities) in nanochannel diodes is based on the determination of the equivalent circuit elements such as the admittance/impedance parameters of their terminals (anode and cathode). The nanochannel diode impedance can be determined by using the 1D Poisson equation in high doped InGaAs semiconductor. Moreover, the analysis of the complex impedance provides an important information about the noise density and the dynamic regime of the diode under applied signal. In addition, the impedance/admittance elements are useful for two main goals calculations:

- the high-frequency noise of the unipolar diodes, especially the current and the voltage spectral densities. For this approach, we use the Nyquist relation which introduces the real part of the admittance/impedance elements.
- the evaluation of the Responsivity and therefore the power generated from signal, which can be used to model the terahertz detectors based on the nanochannel diodes [8].

In Section 2, first the potential in the nanochannel diode is described by 1D Poissons equation and therefore the total current is determined. In particular, the

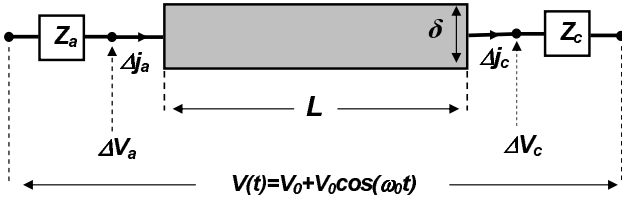


Figure 1: Structure representation of a nanochannel diode of length  $L$  and thickness  $\delta$ . The amplitudes of the anode and cathode are  $\Delta V_a$  and  $\Delta V_c$  respectively.

impedance/admittance can be obtained by the relation between the current density and the potential. Second, the complex admittance/impedance elements are useful for the noise densities calculation, the Responsivity to an applied signal and the noise equivalent power of a channel diodes.

In Section 3, the frequency dependent admittance/impedance matrix is studied and interpreted as a function of the diode geometrical parameters (length and width) and operating temperature.

In Section 4, the noise spectral density is obtained by using the Nyquist relation. Indeed, the diode rectifying properties, the responsivity and the noise equivalent power (NEP), are discussed as a function of different applied voltage (constant and microwave voltage). In the general analysis, the NEP has been considered as an essential factor in the performance of unipolar diode detectors [2].

## 2 Analytical model of channel diode

We consider a nanochannel diode structure reported schematically in Figure 1 where the  $L$  is the length and  $\delta$  is the thickness of diode.

In extension, the total current density along the diode is obtained by the displacement and drift current components as:

$$\Delta j = -\epsilon_c \epsilon_0 \frac{d}{dt} \frac{d\Delta V}{dx} - e\mu n_0 \frac{d\Delta V}{dx} = \gamma \frac{d\Delta V}{dx} \quad (1)$$

Where the  $\mu = \frac{e}{m^* \nu}$  is the material mobility related to the relaxation rate  $\nu$  and the effective mass  $m^*$ ,  $\Delta V$  is the potential along the diode,  $n_0$  is the electron concentration and  $\epsilon_c$  is the dielectric constants of the nanochannel material. By using the Fourier transformation, we obtained the term  $\gamma$  of equation (1) as  $\gamma = -e^2 n_0 / m^* \nu - i\omega \epsilon_c \epsilon_0$ .

The potential distribution  $\Delta V$  is determined through the 1D Poisson equation rewritten as:

$$\frac{d^2 \Delta V}{dx^2} = -\frac{e}{\epsilon_c \epsilon_0} [n_0 - N(x)] \quad (2)$$

Here  $N(x)$  is the effective donor concentration. Also the potential conditions at the diode terminals are defined as  $\Delta V(x=0) = \Delta V_a$  and  $\Delta V(x=L) = \Delta V_c$  for solving Eq. (2). After the resolution of equation (2), the equation (1) is accompanied by an approximated relation between the current and the potential in absence of thermal noise as:

$$\Delta j(\omega) = \frac{G}{L} \Delta V(\omega) \quad (3)$$

Where  $G = \epsilon_c \epsilon_0 \omega_p^2 \alpha^{-1} / (i\omega + \nu)$ ,  $\alpha = \omega_p^2 / (\omega_p^2 + i\omega(i\omega + \nu))$ ,  $\omega_p = \sqrt{e^2 n_0 / \epsilon_c \epsilon_0 m^*}$ . The current along the diode is unidimensional and therefore the admittance expression at the cathode, anode and cathode-anode contacts is  $|Y_{ij}| = \frac{G}{L}$  (where  $ij = a, c$ ), respectively.

The admittance of equation (3) is similar to that calculated for ungated transistor in Ref. [9]. The equation (3) presents the basis for the calculation of the diode impedance components in terahertz frequency as:

$$Y(\omega) = Z^{-1}(\omega) \quad (4)$$

where  $Y(\omega)$  and  $Z(\omega)$  are the admittance and impedance elements, respectively. According to equation (4), the linear response descriptions based on the admittance  $Y(\omega)$  or impedance  $Z(\omega)$  matrixes are equivalent. This condition means that the current/voltage spectral density related to  $Y/Z$  has a similar description which leads to present only the current noise spectrum in the discussion section.

The spectral density of current/voltage fluctuations can be obtained by using the real parts of the admittance/impedance complex components ( $Y(\omega)$  or  $Z(\omega)$ ). In the thermal equilibrium and by using the Nyquist relation, the noise calculations take the form [10]:

$$\begin{aligned} S_{ii}(\omega) &= 4kTR \operatorname{Re}[Y(\omega)] \\ S_{vv}(\omega) &= 4kTR \operatorname{Re}[Z(\omega)] \end{aligned} \quad (5)$$

It should be emphasized that the voltage spectral density  $S_{vv}(\omega)$  is integrated in the noise equivalent power (NEP) calculations under a microwave voltage applied to the diode terminals. In particular, the NEP is partially studied for AlGaN unipolar diode by Monte Carlo simulations in article [2]. The sinusoidal voltage applied to the diode is proportional to  $V = V_{DC} + V_0 \cos(\omega t)$  and the current response  $j(t)$  is rectified to the spectral current representation  $\Delta j(\omega)$  obtained by using equation (3).

For simplicity, the intrinsic Responsivity is determined by the rectified current  $\Delta j(\omega)$  and the resistance of the diode  $R$  as:

$$S_{int}(\omega) = \frac{\Delta j(\omega) \times R(\omega)}{\operatorname{Re}[V_0^2 / 2Z(\omega)]} \quad (6)$$

with  $R(\omega) = Re[Z(\omega)]$  resistance corresponds to the real part of the diode complex impedance  $Z(\omega)$ . Let us note that the impedance  $Z(\omega)$  is extracted from the admittance element described by equation (4).

By using Eqs. (5) and (6), we obtain the intrinsic NEP as the ratio between the voltage spectral density  $S_{vv}(\omega)$  in the diode and the intrinsic Responsivity  $S_{int}(\omega)$ :

$$NEP_{int}(\omega) = \frac{\sqrt{S_{vv}(\omega)}}{S_{int}(\omega)} \quad (7)$$

The Nyquist theorem using for the voltage noise calculation  $S_{vv}(\omega)$  impose the equilibrium condition obtained by the small value of  $DC$  voltage ( $V_{DC} \rightarrow 0$ ). Therefore, we can express the extrinsic  $NEP$  as:

$$NEP_{ex}(\omega) = \frac{\sqrt{S_{vv}(\omega)}}{1 - \left| \frac{Z(\omega) - Z_0}{Z(\omega) + Z_0} \right|^2} \quad (8)$$

The term in the denominator of equation (8) presents the extrinsic Responsivity and  $Z_0$  is the experimental constant impedance of the diode.

In Section 3 and 4, we calculate and discuss the admittance/impedance ( $Y_{ij}/Z_{ij}$ ) and the noise/NEP spectrum of a nanochannel diode, respectively.

### 3 Nanochannel diodes response

We discuss, in this section, the modulus of the admittance and the real part of the impedance as functions of the diode parameters ( $L$  and  $\nu$ ). We consider a InGaAs channel diode with electron concentration  $n_0 = 8 \times 10^{17} \text{ cm}^{-3}$  and a thickness  $\delta = 15 \text{ nm}$ .

Let us note that the admittances of the diode terminals take the same expression  $|Y_{aa}| = |Y_{cc}| = |G/L|$  according to equation (3) which leads to present an admittance of anode terminal. The figure 2 illustrates the modification introduced by the length  $L$  and the relaxation rate  $\nu$  on the anode admittance modulus  $|Y_{aa}|$ . We present in figure 3 the real part of impedance  $Re[Z_{aa}]$  which is widely used for the noise and the intrinsic Responsivity calculations. In the case of Fig. 2, at low frequencies,  $|Y_{aa}|$  demonstrates the Lorentzian shape corresponding to the decrease of  $G$  term in the admittance function. For the real part of impedance, we observe the appearance of one resonance peak near 10 THz corresponding to the plasma frequency  $\omega_p$ . Indeed, the resonance frequency of  $Re[Z_{aa}]$  (near 10 THz) can be compared and interpreted by the expression [10, 11]:

$$f_p = \omega_p \frac{p}{\sqrt{\left(\frac{\lambda L}{\pi}\right)^2 + p}} \quad (9)$$

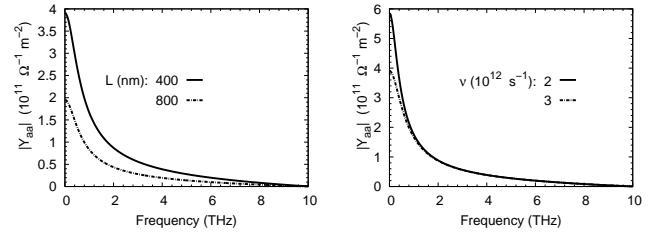


Figure 2: Anode admittance modulus  $|Y_{aa}|$  as functions of the frequency for the reported lengths  $L$  and relaxation rates  $\nu$ .

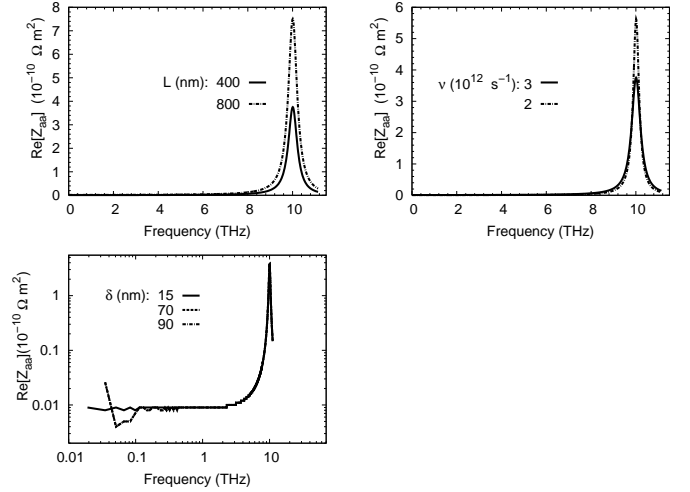


Figure 3: Real part of impedance as functions of the frequency for reported lengths  $L$ , relaxation rate  $\nu$  and thickness  $\delta$ .

where  $p = 1, 2, 3, 4..$  number of excitation and  $\lambda = \sqrt{1/d\delta}$ . The resonance peak of diode impedance spectrum is obtained according to equation (9) when  $\lambda \rightarrow 0$  (for  $d \rightarrow \infty$  ungated transistor corresponding to channel diode structure):

$$f_{res} = \omega_p = const \quad (10)$$

Compared to the plasma resonances of the transistor admittance  $f_p$  (equation (9)), the impedance spectrum exhibits one plasma resonance  $f_{res}$  (equation (10)) explaining the absence of oscillations along the diode channel. It can also be noticed that the amplitude of the resonance peak in figure 3 decreases when the diode length decreases. In low frequency, we observe that the decrease of the length  $L$  tends to increase the amplitude of the admittance modulus. Moreover, for the relaxation rate effect, the value  $3 \times 10^{12}$  corresponding to 300 K can decrease both the resonance peak of  $Re[Z_{aa}]$  and the amplitude of  $|Y_{aa}|$ . The resonance plasma  $f_{res}$  (or  $\omega_p$ ) is related to the relaxation rate through the relation  $\nu = \frac{e}{m^* \mu}$ .

We can remark that the thickness  $\delta$  introduces a

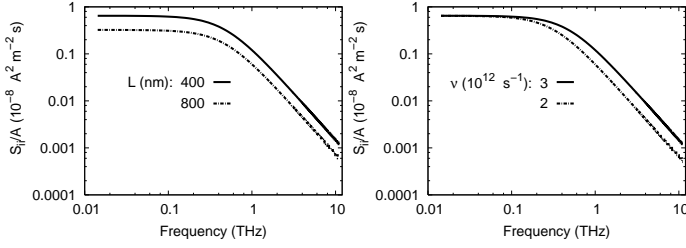


Figure 4: Spectral density of current fluctuation  $S_{ii}(\omega)$  as functions of the frequency for the reported lengths  $L$  and relaxation rate  $\nu$ .

modification on the diode resistance ( $Re[Z_{aa}]$ ) in low frequency range, where the low thickness  $\delta = 15$  nm stabilize the resistance  $R$ .

## 4 Noise and responsivity of channel diodes

In this section we investigate the Noise, the Responsivity and the noise equivalent power of an InGaAs channel diode.

### 4.1 Current noise

The noise spectral densities of current/voltage fluctuations are calculated according to equation (5), in particular, we discuss the current spectral density  $S_{ii}$  which is widely used in the literature. Figure 4 reports the frequency dependence of the spectral current density  $S_{ii}(\omega)$ , proportional to the real part of admittance and obtained through Eq. (5). The spectral density exhibits the usual Lorentzian behavior obtains to diode structures at thermal equilibrium. The results of spectral density are compared to the Lorentz spectrum obtained for the homogenous diode in Ref. [12]. It can be seen that the decreasing of the length  $L$  increases the spectral density due to the increases of the admittance modulus. With the decrease of the relaxation rate  $\nu$ , the noise spectrum decreases in the high-frequency region due to their strongly dependence to the temperature  $T$  compared to the relaxation rate  $\nu$  in real part of admittance according to equation (5).

### 4.2 Responsivity

The Responsivity of channel diodes to a sinusoidal signal  $V(t) = V_{DC} + V_0 \cos(\omega t)$  determined in accordance with equation (6) under equilibrium condition achieved by a small values of  $V_{DC}$  and  $V_0$ . Moreover, we suppose that the dc and ac voltages are equals  $V_{DC} = V_0$  at the frequency  $\omega_0$ , this implies that the applied voltage  $V$  is proportional to

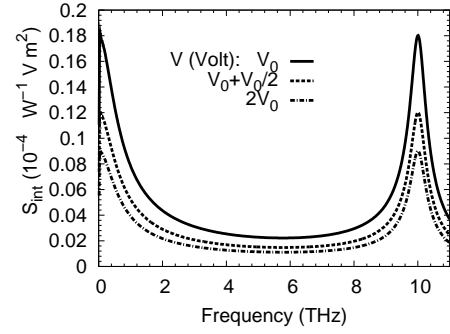


Figure 5: Intrinsic Responsivity  $S_{int}$  for different fixed values of the voltage  $V$  corresponding to different phases of the ac component  $V(t) = V_0 + V_0 \cos(\omega_0 t)$  ( $\omega_0 t = 0, \pi/3, \pi/2$ ). With  $V_0 = 0.25$  V,  $L = 400$  nm,  $\nu = 3 \times 10^{12}$  s $^{-1}$  and electron concentration  $n_0 = 8 \times 10^{17}$  cm $^{-3}$ .

$V(t) = V_0 + V_0 \cos(\omega_0 t)$ . The calculations of the Responsivity will be carried out in two steps. In the first step, the Responsivity is determined for different fixed values of the voltage  $V(t)$  corresponding to different phases of the ac component  $\omega_0 t = 0, \pi/3, \pi/2$  ( $V = 2V_0, V_0 + \frac{V_0}{2}, V_0$ ). Such a choice of voltage values ( $V = 2V_0, V_0 + \frac{V_0}{2}, V_0$ ) includes in equation (3) to extracted the rectified current  $\Delta j(\omega)$  at a certain voltage  $V$ . In the second step, we assume that the voltage takes an adiabatic variation in time  $V(t) = V_0 + V_0 \cos(\omega_0 t)$  where  $\omega_0$  has a finite value 10 GHz. In the case considered here, the variation  $V(t)$  produces the dependence of the Responsivity on the harmonic contribution of the ac signal applied to the diode.

Figure 5 illustrates a frequency behaviour of the Responsivity at absence of harmonics contribution in applied voltage  $V = const$  ( $\omega_0 t = const$ ). The results of figure 5 consist the first step of the Responsivity calculation where  $V_0 = 0.25$  V. The Responsivity in figure 5 is performed under a constant voltage operation  $V$ , when the current flowing through the diode terminals changes its values by a certain time moment  $\omega_0 t = constant$ . We remark that the Responsivity, at low frequencies, demonstrates the Lorentzian shape corresponding to the behavior of the admittance  $Y(\omega)$  (see figure 2), and a peak at frequency 10 THz corresponding to the presence of a resonance peak in real part of impedance (see figure 3). According to equation (6), the Responsivity behavior at low frequencies (Lorentzian form) and near 10 THz (resonance peak) depends to the two parts of ratio  $\frac{V_0^2}{2} Y(\omega)$  and  $R(\omega) = Re[Z(\omega)]$ , respectively. In addition, the decreasing of the voltage  $V$  increases the amplitude of the Responsivity according to equation (6). The diode

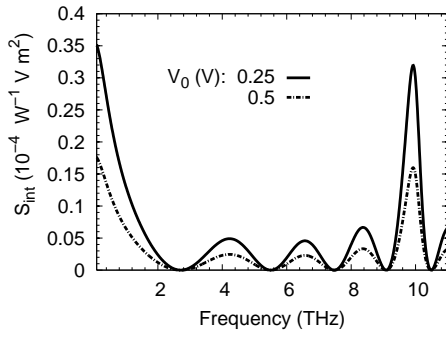


Figure 6: Intrinsic responsivity  $S_{int}$  as functions of ac voltage component  $V_0$ . With  $\omega_0 = 10$  GHz,  $L = 400$  nm,  $\nu = 3 \times 10^{12}$  s $^{-1}$  and carrier concentration  $n_0 = 8 \times 10^{17}$  cm $^{-3}$ .

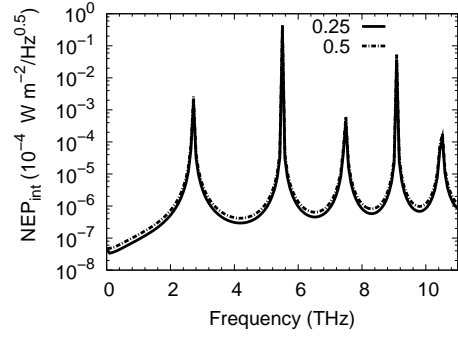


Figure 8: Intrinsic noise equivalent power  $NEP_{int}$  as a function of frequency evaluated for different voltage  $V_0$ . With  $L = 400$  nm,  $\nu = 3 \times 10^{12}$  s $^{-1}$  and  $n_0 = 8 \times 10^{17}$  cm $^{-3}$ .

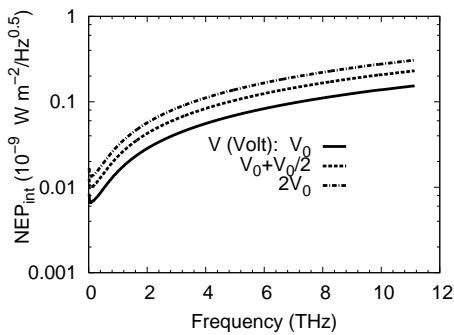


Figure 7: Intrinsic noise equivalent power  $NEP_{int}$  as a function of frequency evaluated for different fixed values  $V$ . With  $V_0 = 0.25$  V,  $L = 400$  nm,  $3 \times 10^{12}$  s $^{-1}$  and  $n_0 = 8 \times 10^{17}$  cm $^{-3}$ .

response behavior under a constant voltage effect has been extensively discussed and explained in Ref. [10].

Figure 6 shows the variation of the Responsivity  $S_{int}(\omega)$  as a function of the ac voltage  $V_0$  under a microwave voltage  $V(t)$  in accordance with Eq. (6).

In the case of Fig. 6, a short series of peaks caused by the microwave excitation along to the diode is placed between the lorentzian behavior and the resonance peak of 10 THz (see fig 5). Moreover, the small value of voltage  $V_0$  leads to increase the amplitude of resonance peaks. As discussed above in Fig. 5, the most important resonance in the series of peaks (see fig 6) is at the frequency 10 THz where the impedance real part effect is dominant.

### 4.3 Intrinsic noise equivalent power

In this section, we represent the frequency dependence of the intrinsic noise equivalent power  $NEP_{int}$  obtained through Eq. (7). The intrinsic NEP is determined for two case of excitation, under a constant and

microwave voltage  $V$  applied between the diode terminals, described above in the section of Responsivity. For the first calculations, the intrinsic Responsivity in equation (7) corresponds to the results of fig 5. Figure 7 presents the modification introduced to the intrinsic NEP by different fixed values of the voltage  $V$  corresponding to  $2V_0$ ,  $\frac{3V_0}{2}$ ,  $V_0$ . In fig 7, the quality of the intrinsic  $NEP$  increases when the voltage  $V$  increase to  $2V_0$ . According to equation (7) the behavior of the intrinsic  $NEP$  is inversely proportional to the voltage  $V_0$  dependence as discussed in fig 5.

Figure 8 shows the frequency-dependent of the intrinsic  $NEP$  to the microwave signal  $V(t)$  for different  $V_0$ . The harmonic excitation applied to the diode appears as resonance peaks in the intrinsic  $NEP$  spectrum. Originally, resonances that appeared on the intrinsic  $NEP$  due to the responsivity behavior in fig 6. Indeed, increasing the voltage  $V_0$  induces an increasing of  $NEP$  amplitude without shifts of the resonance frequencies. This final discussion shows that the variation of the intrinsic noise equivalent power depends to the voltage drop on the diode terminals.

### 4.4 Extrinsic noise equivalent power

Let remark equation (8), the extrinsic  $NEP$  depends strongly to the parameters (length, thickness and relaxation rate) and the response of diode. According to the voltage spectral density approximation  $S_{vv}$  in equation (8), the extrinsic  $NEP$  reflect the diode behavior such as the impedance response. The extrinsic  $NEP$  shows in figure 9 for InGaAs channel diodes. The results reported for different lengths and relaxation rate values. The noise power spectrum exhibits a resonance peak near 10 THz corresponding to the high value of diode resistance (see fig 3). Moreover, the decrease of the diode length decrease the res-

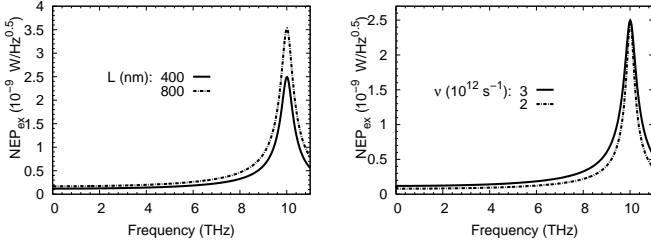


Figure 9: Extrinsic  $NEP$  as functions of the frequency for reported length  $L$  and relaxation rate  $\nu$ . With  $\delta = 15$  nm,  $n_0 = 8 \times 10^{17}$  cm $^{-3}$ .

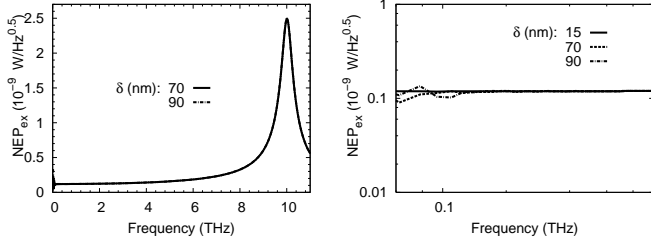


Figure 10: Extrinsic  $NEP$  as functions of the frequency for different thickness  $\delta$ . With  $L = 400$  nm,  $\nu = 3 \times 10^{12}$  s $^{-1}$  and  $n_0 = 8 \times 10^{17}$  cm $^{-3}$ .

onance quality of the extrinsic  $NEP$  amplitude, that is by the decrease of impedance real part (see figure 3). In low frequency, the extrinsic  $NEP$  decrease by the decreasing of the relaxation rate. This effect is due to the decrease of the temperature which decreases the voltage spectral density  $S_{vv}$  for a small perturbation associated to low frequency.

Figure 10 illustrates the frequency dependence of extrinsic  $NEP$  of InGaAs channel diode calculated by using Eq. (8), for the thickness 15, 70 and 90 nm. The diode thickness takes effect in low frequency according to figure 10 when the resonance peak appears near 10 THz for the nano-diode with length 400 nm and high electron concentration  $8 \times 10^{17}$  cm $^{-3}$ . Compared with figure 11, the appearance of the resonance peak is near 1.8 THz for the AlGaIn micrometer diode with low electron concentration  $10^{17}$  cm $^{-3}$ . Therefore, the diode electron surface density effect is considered on the plasma frequency term  $\omega_p$  when the electron concentration produces the correct behavior of the diode in high frequency. In figure 10, the width  $\delta = 15$  nm gives a constant  $NEP$  up to 1 THz when the high width value 90 nm increases the  $NEP$  in gigahertz frequency. The surface ( $L \times \delta$ ) introduces an increasing on the diode resistance ( $Re[Z(\omega)]$ ) and leads to obtained a poorer high frequency behavior.

For figure 11, we use the analytical model for extrinsic  $NEP$  calculation of the AlGaIn diode studied in Ref [2]. The analytical simulations in figure 11 is

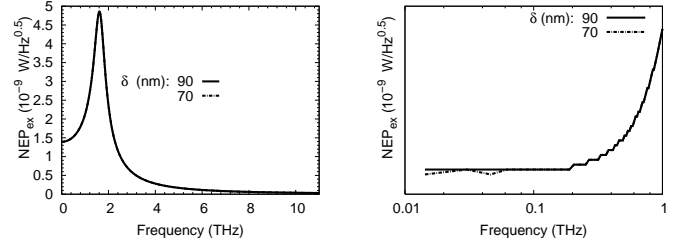


Figure 11: Extrinsic  $NEP$  of an AlGaIn unipolar diode calculated for different thickness  $\delta$ , with  $L = 1$   $\mu$ m,  $\mu = 1200$  cm $^2$ /V.s,  $\nu = 5 \times 10^{12}$  s $^{-1}$  and  $n_0 = 10^{17}$  cm $^{-3}$

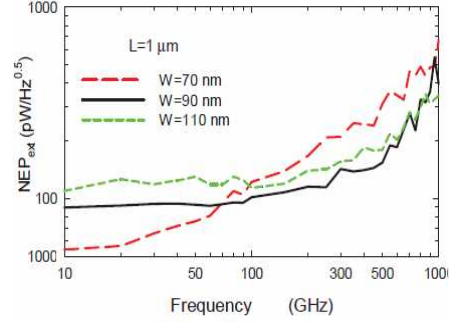


Figure 12: Extrinsic  $NEP$  by Mont Carlo calculations of 16 AlGaIn nanochannel in parallel. The results are for different thickness  $\delta$  with length is fixed to 1  $\mu$ m. The mobility  $\mu = 1200$  cm $^2$ /V.s,  $\nu = 5 \times 10^{12}$  s $^{-1}$  and  $n_0 = 10^{17}$  cm $^{-3}$

for the AlGaIn unipolar diode with 1  $\mu$ m length and  $10^{17}$  cm $^{-3}$  electron concentration.

It should be emphasized that the good agreement found between analytical and MCP results obtained in Ref. [2], in the gigahertz frequency range. Indeed, the figure 11 presents a resonance peak near 1.8 THz obtained by the micrometer diode with low electron concentration.

The following discussions can extract:

- The high electron mobility of semiconductor as InGaAs gives a high frequency response of detector compared to AlGaIn semiconductor.
- The high electron concentration can increase the frequency resonance peak in the  $NEP$  since  $\omega_p \propto \sqrt{n_0}$ , which increases the frequency range of detectors.
- The diode geometry introduces an optimization of the noise equivalent power amplitude, since the diode surface (length and thickness) gives a significant increasing of the diode response (admittance modulus) and resistance ( $Re[Z(\omega)]$ ).

- The contribution of the applied voltages is accounted for the intrinsic detector parameters: responsivity and the noise equivalent power where the microwave voltage leads to appear a supplementary harmonics resonances.

## 5 Conclusion

An Extension of analytical calculations based on the transistor model with the consideration distance channel-gate tends to infinity, is useful in this article to determine the response and the noise equivalent power of the nanochannel diodes.

The calculation of the admittance elements can determine the complex impedance where their real part presents the diode resistance. The impedance spectrum exhibits a peak near 10 THz corresponding to frequency plasma resonance. The diode response explains the behavior of terahertz detector, since the impedance factor is integrated in the voltage spectral density  $S_{vv}$ , the intrinsic Responsivity  $S_{int}$  and the noise equivalent power  $NEP$  expressions.

The discussion of the length and the relaxation rate effects on the diode response and the voltage noise leads to perform the diode geometry for a special frequency range detection. An increase of the diode length increases the extrinsic noise power  $NEP$  amplitude and keep the frequency resonance peak while the diode thickness effect takes place in the low frequency and introduces an increasing of the  $NEP_{ext}$ . The resistance of the diode ( $Re[Z(\omega)]$ ) decreases when the relaxation rate increase and therefore increases the extrinsic  $NEP$  in gigahertz frequency. We let not that has no effect of the diode geometry and the relaxation rate on the resonance plasma frequency  $\omega_p$  which depends only to the electron concentration.

The intrinsic Responsivity  $S_{int}$  and noise power  $NEP_{int}$  show a significant dependence on the applied voltage according to their analytical expression. The Responsivity spectrum exhibits a lorentzian form in low frequency and a resonance peak near 10 THz for a constant voltage condition applied between the diode terminals. A sinusoidal voltage applied to the diode introduces a supplementary resonances due to the harmonic contribution of the signal and leads to obtain a series of peaks in the  $NEP_{int}$  spectrum. These peaks explain the frequencies detected by the nanochannel diodes.

**Acknowledgements:** The research was supported by the University of Montpellier, France in the case of the third author.

## References:

- [1] I. I. la Torre, J. Mateos, D. Pardo, and T. Gonzalez, "Monte carlo analysis of noise spectra in self-switching nanodiodes," *Appl. Phys. Lett.*, vol. 103, p. 024502, 2008.
- [2] J.-F. Millithaler, I. I. de-la Torre, T. Gonzalez, J. M. P. Sangar, G. Ducournau, and C. Gaquire, "Noise in terahertz detectors based on semiconductor nanochannels," *IEEE proceeding*, vol. DOI:978-1-4799-0671-0/13, 2013.
- [3] C. Balocco and al, "Room-temperature operation of a unipolar nanodiode at terahertz frequencies," *Journal of Applied Physics Letter*, vol. 98, p. 223501, 2011.
- [4] I. Cortes-Mestizo, V. H. Mndez-Garca, J. Briones, M. P.-C. R. Droopad, S. McMurtry, M. Hehn, F. Moutaigne, and E. Briones, "Terahertz harvesting with shape-optimized inalas/ingaas self-switching nanodiodes," *AIP ADVANCES*, vol. 5, p. 117238, 2015.
- [5] C. B. et al, "Low-frequency noise of unipolar nanorectifiers" *Appl. Phys. Lett*, vol. 99, p. 113511, 2011.
- [6] A. M. Song, M. Missous, A. R. Peaker, L. Samuelson, and W. Seifert, "Unidirectional electron flow in a nanometer-scale semiconductor channel: A self-switching device," *Applied Physics Letters*, vol. 83, p. 1881, September 2003.
- [7] A. Song, I. Maximov, M. Missousa, and W. Seifert, "Low-dimensional systems and nanostructures," *Physica E*, vol. 21, 2004.
- [8] N. K. Dhar, R. Dat, and A. K. Sood, *Optoelectronics Advanced Materials and Devices*, vol. DOI: [10.5772/51665], 2013.
- [9] H. Marinchio, C. Palermo, L. Varani, P. Shiktorov, E. Starikov, and V. Gruzinskis, "Suppression of high-frequency electronic noise induced by 2d plasma waves in field-effect and high-electron-mobility transistors," *IEEE proceeding*, vol. DOI: 978-1-4577-0191-7/11, 2011.
- [10] E. Starikov, P. Shiktorov, and V. Gruzinskis, "Investigation of high-frequency small-signal characteristics of FETs/HEMTs," *Semicond. Sci. Technol.*, vol. 27, p. 045008, 2012.
- [11] H. Marinchio, J.-F. Millithaler, C. Palermo, L. Varani, L. Reggiani, P. Shiktorov, E. Starikov,

and V. Gružinskis, "Plasma resonances in a semiconductor slab of arbitrary thickness," *Appl. Phys. Lett.*, vol. 98, p. 203504, 2011.

- [12] F. Mahi, A. Helmaoui, L. Varani, P. Shiktorov, E. Starikov, and V. Gruzinskis, "Calculation of the intrinsic spectral density of current fluctuations in nanometric schottky-barrier diodes at terahertz frequencies," *Physica B*, vol. 403, pp. 3765–3768, 2008.